



SACRED HEART RESEARCH PUBLICATIONS

# Journal of Functional Materials and Biomolecules

Journal homepage: [www.shcpub.edu.in](http://www.shcpub.edu.in)



ISSN: XXXX-XXXX

## Probing the Electrochemical Reactions in Li Battery Materials Employing Magnetization Measurements

Collin Issac Thomas<sup>1</sup> and K. Kamala Bharathi<sup>1,\*</sup>

Received on 19 Dec 2016, Accepted on 07 Apr 2017

### Abstract

We report on utilization of magnetization measurements as a tool to investigate the cathode/anode materials after they are electrochemically charged and discharged. We have performed the *ex-situ* magnetic studies on the  $\text{CoFe}_2\text{O}_4$  electrodes after 1<sup>st</sup> discharge, 1<sup>st</sup> cycle, 20 and 30 cycles to understand the chemical reactions taking place during the electrochemical cycling. Nanocrystalline cobalt ferrite particles were synthesized by a sol-gel combustion method.  $\text{CoFe}_2\text{O}_4$  is found to crystallize in inverse spinel structure belonging to Fd-3m space group without any impurity phase.  $\text{CoFe}_2\text{O}_4$  electrodes were prepared with PVDF and alginate binders separately and electrochemical cycling was performed on all of them. RT magnetization measurements were carried out on the electrodes after 1<sup>st</sup> discharge, 1<sup>st</sup> cycle, 20 cycles and 30 cycles. Saturation magnetization ( $M_s$ ) of pure  $\text{CoFe}_2\text{O}_4$  powder is seen to be 77 emu/g. In the case of  $\text{CoFe}_2\text{O}_4$ -PVDF electrodes, saturation magnetization values after 1<sup>st</sup> discharge, 1<sup>st</sup> cycle and 30 cycles are 135, 97 and 43 emu/g respectively. Saturation magnetization value of  $\text{CoFe}_2\text{O}_4$ -alginate electrodes after 1<sup>st</sup> discharge, 1<sup>st</sup>, 20<sup>th</sup> and 30<sup>th</sup> cycles is seen to be 130, 63, 60 and 62 emu/g respectively. Obtained results indicate magnetization measurements can help to identify the chemical reactions taking place during the electrochemical cycles in the electrode materials containing magnetic elements.

**Key words:** Sol-gel combustion method, Magnetization measurements, Electrochemical cycling.

### 1 Introduction

Lithium batteries with an operating voltage of ~3.6-4 V are extensively used as a power sources for portable electronic devices such as laptops, cell phones, etc [1-3]. In most of the commercial batteries,  $\text{LiCoO}_2$  and graphite are used as a cathode and anode material respectively [4-6]. The graphite based anode material has already reached its theoretical capacity and the search for alternative anode materials has become the pressing need for several research groups. Layered two dimensional structure or 3D networks of oxides like  $\text{Fe}_2\text{O}_3$ ,  $\text{TiO}_2$ , NiO,  $\text{SnO}_2$ , CuO, in which Li can intercalate reversibly into the lattice without

destroying the crystal structure are extensively studied as an alternative for anode material [7-11]. In addition to that, possibilities of employing the Fe-based ferrites ( $\text{NiFe}_2\text{O}_4$ ,  $\text{CoFe}_2\text{O}_4$ ,  $\text{ZnFe}_2\text{O}_4$ , etc.) as anode material have been explored by few research groups [12-14]. However, Capacity fading during the initial few cycles is one of the challenging problem in ferrite based anodes [12-14].

Co ferrite (CFO) is a ferromagnetic material, crystallizes in inverse spinel structure with the space group of Fd-3m [15,16]. In inverse spinel structure, oxygen ions form face centered cubic (FCC) lattice and the tetrahedral (A) sites are occupied by the  $\text{Fe}^{3+}$  ions and the octahedral sites (B) are occupied by the divalent metal ions ( $\text{M}^{2+}$ ) and  $\text{Fe}^{3+}$ , in equal proportions [15, 16].

Materials with nano dimensions (nanoparticles, nanorods, nanowires) have attracted enormous attention for their enhanced electrochemical properties and interesting behaviors applied in Li battery research field [17-20]. Due to high surface area and very fast redox reactions, battery capability and other electrochemical behaviors are highly influenced by nano materials.

After the electrochemical test, finding out the structural changes in the cathode or anode material employing XRD measurements is very difficult and challenging in the battery research field due to the presence of binder materials in the electrodes. In the present case, we made an attempt to utilize the magnetization measurements as a tool to investigate the cathode/anode materials after they are electrochemically charged and discharged. We have performed the *ex-situ* magnetic studies on the electrodes after 1<sup>st</sup> discharge, 1<sup>st</sup> cycle, 20 and 30 cycles to understand the chemical reactions taking place during the electrochemical cycling. Effect of different binders (polyvinyl pyrrolidone (PVP), polyvinylidene fluoride (PVDF), poly acrylic acid (PAA) and carboxymethyl cellulose (CMC)) on electrochemical properties of electrodes have been reported by several research groups [21-23]. In the present case, we have employed PVDF and alginate binders to prepare the electrodes and made an attempt to explore the structural changes through magnetization studies in each electrode after the

\* Corresponding author: E-mail: [kamalabharathi.k@ktr.srmuniv.ac.in](mailto:kamalabharathi.k@ktr.srmuniv.ac.in)  
Phone: +9677641987

<sup>1</sup> Department of Physics and Nanotechnology, Research Institute, SRM University, Kattankulathur, Chennai 603203, India

electrochemical cycling of CFO anodes. The results obtained are presented and discussed in this paper.

## 2 Experimental

### 2.1 Material synthesis

Nanocrystalline cobalt ferrite CFO particles were synthesized by a sol-gel combustion method. Ni (NO<sub>3</sub>)<sub>2</sub>·6H<sub>2</sub>O, Fe (NO<sub>3</sub>)<sub>3</sub>·9H<sub>2</sub>O, citric acid and urea were used as precursors to synthesize nanocrystalline CoFe<sub>2</sub>O<sub>4</sub> particles. First, the stoichiometric solutions of all the required precursors were mixed with continuous stirring at RT and at 80°C to form a gel, which was then heated up to 180°C. The amorphous powders were collected and pure nano crystalline CoFe<sub>2</sub>O<sub>4</sub> particles were obtained by annealing the powders at 600°C for 3 h.

### 2.2 Characterization

Structural characterization at room temperature (RT) was performed by obtaining the powder X-ray diffraction (XRD) patterns employing Cu-K $\alpha$  radiation (1.54 Å). The measurements were performed employing a PANalytical (X'pert PRO) X-ray diffractometer. Particle size and morphology analysis were characterized employing a field emission scanning electron microscope (FE-SEM Hitachi S-4800, Japan) and a transmission electron microscope with energy dispersive spectroscopy (TEM), JEOL 2010F HRTEM, Japan, with a 200 kV operating voltage. The Raman spectra of powders were recorded at RT employing a HR 800 Raman spectrophotometer (Jobin Yvon- Horiba, France) using monochromatic He-Ne LASER (632.8 nm), operating at 20 mW.

The electrochemical studies of the synthesized CoFe<sub>2</sub>O<sub>4</sub> nanoparticle were analyzed in a CR2032 coin cells. The composite electrode was prepared by mixing 70 wt. % of active material with 20 wt. % Super P carbon black and 10 wt. % PVDF and sodium alginate binders in suitable solvent. The obtained slurry was coated on a piece of copper foil and cut into 12 mm diameter circular electrodes. Lithium foil was used as anode and 1 M solution of LiPF<sub>6</sub> in ethylene carbonate and dimethyl carbonate (1 : 1) was used as the electrolyte. Coin cells were assembled in an argon-filled dry glove box (M. O. Tech) using Whatman GF/D borosilicate glass-fiber separator. Magnetization measurement was carried out at RT employing a vibrating sample magnetometer (VSM, LakeShore 7407). After the Electrochemical cycles, materials were removed from the electrodes and the obtained powders were used for the magnetization measurements.

## 3. Results and Discussion

### 3.1 Structural characteristics and surface morphology

Figure 1 shows the Rietveld refined [24] XRD patterns of the pure CFO powders recorded at RT. CFO is found to crystallize in inverse spinel structure belonging to Fd-3m space group without any impurity phase. Rietveld refinement was carried out on the XRD data obtained at RT using the GSAS program. The wrp (weighted refined

parameter) and the  $\chi^2$  (goodness of the fit) values of the fitting are 4% and 1.00 respectively.

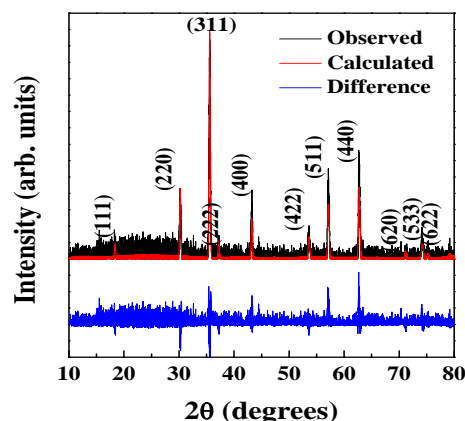


**Fig1.** Rietveld refined XRD pattern of CoFe<sub>2</sub>O<sub>4</sub> powders. Calculated and difference curves are also shown. Formation of inverse spinel phase without any impurities is evident.

The calculated lattice constants  $a=b=c$  values at RT is 13.854 Å ( $\pm 0.002$  Å), which agrees well with the reported value (JCPDS Card No 22-1086) [15]. Figure 2 shows the (SEM image) morphology of the sample. It is clear that the nanocrystalline particles are uniformly distributed. The crystallite size ( $D$ ) was calculated from the integral width of the diffraction lines using the well-known Scherrer's equation after background subtraction and correction for instrumental broadening. The Scherrer equation is: [25]

$$D = 0.9\lambda / \beta \cos\theta, \quad \{1\}$$

where  $D$  is the size,  $\lambda$  is the wavelength of the filament used in the XRD machine,  $\beta$  is the width of a peak at half of its intensity, and  $\theta$  is the angle of the peak. The average grain sizes was found to be  $\sim 25$  nm.

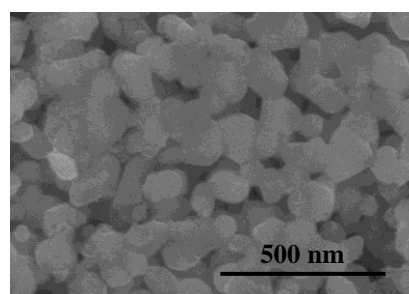


**Fig 2** SEM image of CoFe<sub>2</sub>O<sub>4</sub> particles. Uniform distribution of nano particles is clearly seen.

### 3.2. Raman spectroscopy studies

Figure 3 shows the Raman spectra of CFO powder recorded at RT. Raman spectra showed five active modes of (A<sub>1g</sub> + E<sub>g</sub> + 3F<sub>2g</sub>) and the peaks were observed for CFO at 302.34 cm<sup>-1</sup>, 460.38 cm<sup>-1</sup>, 577.60 cm<sup>-1</sup>, 615.88 cm<sup>-1</sup> and at 690.63 cm<sup>-1</sup>. The peaks corresponding to the wave numbers of 660cm<sup>-1</sup> to 720cm<sup>-1</sup> indicate tetrahedral group and that between 460 cm<sup>-1</sup> to 660 cm<sup>-1</sup> indicate octahedral group of ferrites [26].

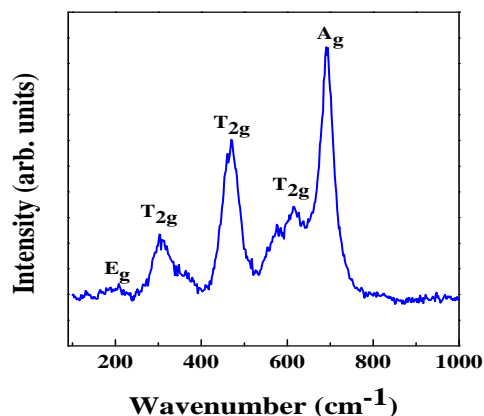


**Fig 3** Room temperature Raman spectra of  $\text{CoFe}_2\text{O}_4$  powders

### 3.3. Magnetic properties

CFO electrodes were prepared with PVDF and alginate binders separately and electrochemical cycling was performed on all of them. RT XRD and magnetization measurements were carried out on the electrodes after 1<sup>st</sup> discharge, 1<sup>st</sup> cycle, 20 cycles and 30 cycles.

During the 1<sup>st</sup> discharge, CFO reacts with the Li ions and convert into Co and Fe nanoparticles along with an amorphous  $\text{Li}_2\text{O}$  phase. However, in the reverse oxidation process (completion of 1<sup>st</sup> cycle), Co and Fe nanoparticles are oxidized to  $\text{CoO}$  and  $\text{Fe}_2\text{O}_3$  phases respectively. Conversion redox mechanism may occur in the following steps [13]

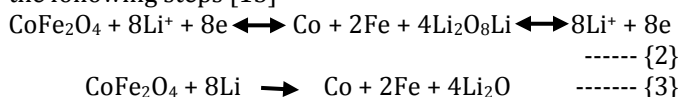
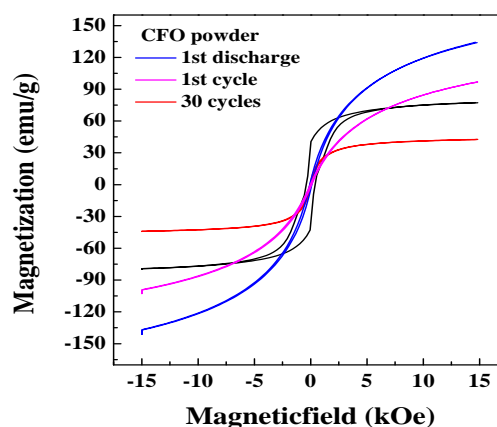
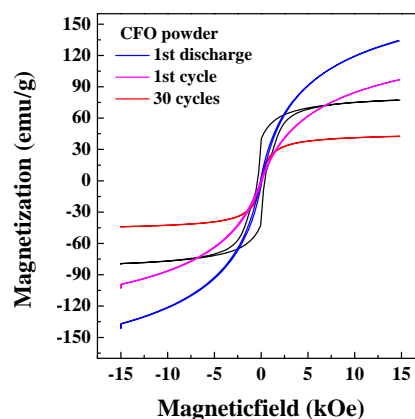


Figure 4 and 5 shows the RT magnetization curves of CFO-PVDF and CFO-alginate electrodes respectively with compared to pure CFO powders. Magnetic moment is seen to be unsaturated even at 15 kOe for all the cases and the magnetic moment at 15 kOe is represented as saturation magnetization ( $M_s$ ) here after. Saturation magnetization ( $M_s$ ) of pure CFO powder is seen to be 77 emu/g, which is agreeing well with the reported values indicating the formation of CFO in pure phase. In the case of CFO-PVDF electrodes, saturation magnetization values after 1<sup>st</sup> discharge, 1<sup>st</sup> cycle and 30 cycles are 135, 97 and 43 emu/g respectively (Table I).

Electrochemical cycles	Saturation magnetization $M_s$ (emu/g)	
	CFO - PVDF	CFO - Alginate
1 <sup>st</sup> Discharge	135	130
1 <sup>st</sup> Cycle	97	63
20 cycles	-	60
30 cycles	43	62

$M_s$  value after 1<sup>st</sup> discharge (135 emu/g) is seen to be higher than that of pure CFO powder (80 emu/g).



**Fig 4** Room temperature magnetization curves of CFO-PVDF electrodes after 1<sup>st</sup> discharge, 1<sup>st</sup> and 30<sup>th</sup> cycles compared with the pure CFO powders. Saturation magnetization is seen to decrease with increasing cycle numbers.

$M_s$   $M_s$  values after the electrochemical cycling's can be explained as follows. After the 1<sup>st</sup> discharge, nanoparticle of Fe and Co along with amorphous  $\text{Li}_2\text{O}$  is present in the electrode. Exchange interaction between the Fe and Co magnetic moments might be complicated in the disordered discharged electrode due to the presence of amorphous  $\text{Li}_2\text{O}$ . Few moments might couple parallel to each other and few might couple anti-parallel to each other. Therefore, the net magnetization is expected to be less than the sum of pure Fe and Co moments. Reported  $M_s$  values for pure Fe and Co are 221 and 162 emu/g respectively [27]. Observed  $M_s$  value after 1<sup>st</sup> discharge is seen to be in between the pure Fe and Co  $M_s$  values and higher than that of pure CFO powder (80 emu/g), clearly indicating the formation of Fe and Co nanoparticles. After the completion of 1<sup>st</sup> cycle, Fe and Co nanoparticles are oxidized to  $\text{Fe}_2\text{O}_3$  and  $\text{CoO}$  phases respectively. Nanoparticles of  $\text{Fe}_2\text{O}_3$  and  $\text{CoO}$  are reported to be very weak ferromagnetic materials

with feeble  $M_s$  ( $\approx 1$  emu/g) values.<sup>28,29</sup> In the present case, the  $M_s$  value after 1<sup>st</sup> cycles is seen to be higher (97 emu/g) than that of  $Fe_2O_3$  and CoO nano particles. Lavela *et.al* [30] have reported the temperature variation of Mossbauer spectroscopy studies on  $CoFe_2O_4$  electrodes after fully charged and discharged states. From the changes in the hyperfine parameters, they have observed the formation of metal particles in fully charged and discharged states with the particle size of 4.5 to 7 nm and their super paramagnetic behaviour. In the present case, nano sized metal particles of Fe and Co might not have completely converted into oxides after the completion of 1<sup>st</sup> cycle, leading to larger observed  $M_s$  value.  $M_s$  value is seen to decrease continuously with increasing electrochemical cycles and its value is seen to be 43 emu/g after 30 cycles. The weak interface and interaction between the CFO and PVDF binders with increasing number of cycles resulted in weakening the exchange interaction and continuous decrease of magnetic moments.

Figure 5 shows the magnetization curves of CFO-alginate electrodes after 1<sup>st</sup> discharge, 1<sup>st</sup>, 20<sup>th</sup> and 30<sup>th</sup> cycles.  $M_s$  value after 1<sup>st</sup> discharge is seen to be 130 emu/g, which is almost same as the CFO-PVDF electrode saturation magnetization value. The  $M_s$  value is seen to decrease to 63 emu/g after the completion of 1<sup>st</sup> cycle and almost same value with increasing the number of cycles (cycle 20 and 30). The strong bonding and stable interface between the CFO and alginate binders even after several cycles resulted in constant specific capacity and  $M_s$  values is clearly evident. Magnetization loops are seen to be very narrow after charging and discharging the electrodes. Due to the very small particle size, each particle behaves as a single domain resulted in superparamagnetic like behavior.

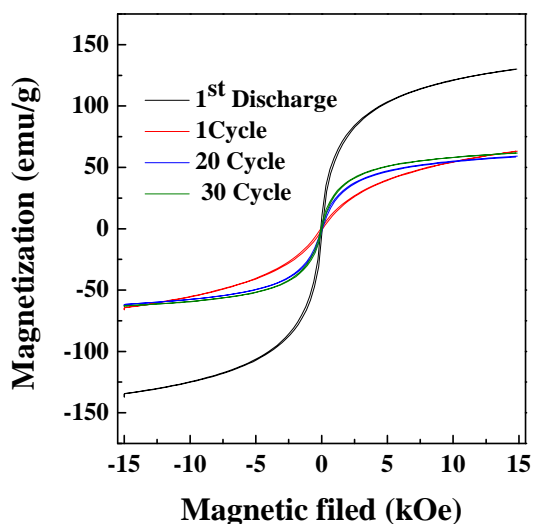


**Fig 5** Room temperature magnetization curves of CFO-alginate electrodes after 1<sup>st</sup> discharge, 1<sup>st</sup>, 20<sup>th</sup> and 30<sup>th</sup> cycles compared with the pure CFO powders. Saturation magnetization is seen to be almost constant with increasing cycle numbers.

#### 4 Conclusions

In summary, *ex-situ* magnetic studies on the  $CoFe_2O_4$  electrodes after the electrochemical cycling helps to understand the chemical reactions taking place during the electrochemical cycling. Nanocrystalline  $CoFe_2O_4$  particles were synthesized by a sol-gel combustion method and found to crystallize in inverse spinel structure with lattice constants  $a=b=c$  values at RT is 8.354 Å ( $\pm 0.002$  Å). Raman spectra showed five active modes of ( $A_{1g} + E_g + 3F_{2g}$ ) and the peaks corresponding to the wave numbers of 660 $cm^{-1}$  to 720 $cm^{-1}$  indicate tetrahedral group and that between 460  $cm^{-1}$  to 660  $cm^{-1}$  indicate octahedral group of ferrites.  $CoFe_2O_4$  electrodes were prepared with PVDF and alginate binders separately and electrochemical cycling was performed on all of them. RT magnetization measurements were carried out on the electrodes after 1<sup>st</sup> discharge, 1<sup>st</sup> cycle, 20 cycles and 30 cycles. In the case of  $CoFe_2O_4$ -PVDF electrodes, saturation magnetization values after 1<sup>st</sup> discharge, 1<sup>st</sup> cycle and 30 cycles are 135, 97 and 43 emu/g respectively. Saturation magnetization value of  $CoFe_2O_4$ -alginate electrodes after 1<sup>st</sup> discharge, 1<sup>st</sup>, 20<sup>th</sup> and 30<sup>th</sup> cycles is seen to be 130, 63, 60 and 62 emu/g respectively. Saturation magnetization values obtained after the electrochemical measurements helps to identify the chemical reactions taking place in the electrode materials containing magnetic elements.

#### References

- [1] M. A. Darwish, S. A. Saafan, D. El- Kony, N. A. Salahuddin, J. Magn. Mater, 385, (2015) 99.
- [2] S. T. Assar, H.F. Abosheisha, M. K. El Nimr, J. Magn. Mater, 354, (2014) 1.
- [3] M. Armand, J. M. Tarascon, Nature, 451, (2008) 652.
- [4] M. V. Reddy, G. V. Subba Rao, and B. V. R. Chowdari, Chem. Rev., 113, (2013) 5364.
- [5] M. Wakihara, O. Yamamoto, Eds. Li-Ion Batteries; Wiley-VCH: New York, 1998.
- [6] W. A. Van Schalkwijk, B. Scrosati, Eds. Advances in Lithium-Ion Batteries; Kluwer Academic /Plenum: New York, 2002.
- [7] P. S. Veluri and S. Mitra, RSC Adv., 3, (2013) 15132 .
- [8] W. Wang, Q. Sa, J. Chen, Y. Wang, H. Jung, and Y. Yin, ACS. Appl. Mater. Interfaces, 5, (2013) 6478.
- [9] H. Liu, G. Wang, J. Liu, S. Qiao and H. Ahn, J. Mater. Chem., 21, (2011) 3046 .
- [10] D. Su, H. J. Ahn and G. Wang, Chem. Commun., 49, (2013) 3131.
- [11] B. Wang, X. L. Wu, C. Y. Shu, Y. G. Guo and C. R. Wang, J.Mater.Chem., 20, (2010) 10661 .
- [12] Y. Ding, Y. Yang, H. Shao, power sources, 244, (2013) 610 .
- [13] P. Ramesh Kumar and S. Mitra, RSC Adv., 3, (2013) 25058 .
- [14] R. Alcantara, M. Jaraba, P. Lavela and J. L. Tirado, Chem. Mater., 14, 2847 (2002)
- [15] J. Smith and H. P. J. Wijn, *Ferrites*, Philips Technical Library, (Eindhoven-Holland, 1965)

- [16] K. Kamala Bharathi, M. Noor-A-Alam, R. S. Vemuri and C. V. Ramana, *RSC Adv.*, 2, (2012)941 .
- [17] H. W. Lee, P. Muralidharan, R. Ruffo, C. M. Mari, Y. Cui, and D. K. Kim, *Nano Lett.*, 10, (2010) 3852.
- [18] K. M. Shaju, F. Jiao, A. Debart, P. G. Bruce, *Phys. Chem. Chem. Phys.*, 9, (2007)1837.
- [19] N. Li, C. J. Patrissi, G. Che, C. R. Martin, *J. Electrochem. Soc.* 147, (2010) 2044.
- [20] Y. Wang, G. Z. Cao, *Chem. Mater.*, 18, (2006) 2787.
- [21] S. Bridel, T. Azais, M. Morcrette, J. M. Tarascon and D. Larcher, *Chem. Mater.*, 22, (2010) 1229.
- [22] D. Mazouzi, B. Lestriez, L. Roue and D. Guyomard, *Electrochem. Solid-State Lett.*, 12, (2009)A215.
- [23] A. Magasinski, B. Zdyrko, I. Kovalenko, B. Hertzberg, R. Burtovyy, C. F. Huebner, T. F. Fuller, I. Luzinov and G. Yushin, *ACS Appl. Mater. Interfaces*, 2, (2010)3004.
- [24] A. C. Larson and R. B. Von Dreele, General Structure Analysis System (GSAS), Los Alamos National Laboratory Report LAUR 86 (2004)748
- [25] A. L. Patterson, *Phys. Rev.*, 56, (1939) 978.
- [26] G. Dixit, L. P. Singh, R. C. Srivastava, H. M. Agrawal, R. J. Choudury, *Adv. Mat. Lett.* 3, (2009) 21
- [27] S. Chikazumi, *Physics of ferromagnetism* (Oxford University Press, New York 1997)
- [28] R. Skomski, J. M. D. Coey, *Permanent Magnetism*, Institute of Physics Publishing Ltd. 1999.
- [29] A. Tomou, D. Gournis, I. Panagiotopoulos, Y. Huang, G. C. Hadjipanayis, B. J. Kooi, *J. Appl. Phys.*, 99, (2006)123915.
- [30] P. Lavela, J. L. Tirado, M. Womes and J. C. Jumas, *J. Phys. Chem. C*, 113, (2009)20081.